

AD 741227

SEMIANNUAL REPORT 10-MICROMETERS DETECTOR

ARPA Order No. 1806

Contract No. N00014-70-C-0161
(Modification P00003)

Program Code No. 1E90K21
Investigators: W. Chiou, M. Aita,
A. Vitolo, and F. Pace
(516) 595-4211

Contractor:
AIL, a division of CUTLER-HAMMER
Deer Park, New York 11729

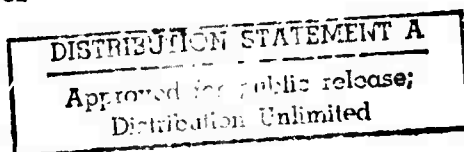
Scientific Officer:
Director, Physics Programs
Physical Science Division
Office of Naval Research

Effective Date of Contract: 1 June 1971
Contract Expiration Date: 31 May 1972
Amount of Contract: \$99,361

Sponsored by Advanced Research
Projects Agency, ARPA Order No. 306

This research was supported by the Advanced Research Project
Agency of the Department of Defense and was monitored by ONR
under Contract No. N00014-70-C-0161.

Reproduced by
NATIONAL TECHNICAL
INFORMATION SERVICE
Springfield, Va. 22151



AIL a division of
CUTLER-HAMMER
DEER PARK, LONG ISLAND, NEW YORK 11729

D D C
RECEIVED
MAY 9 1972
C

SEMIANNUAL REPORT 10-MICROMETERS DETECTOR

ARPA Order No. 1806

**Contract No. N00014-70-C-0161
(Modification P00003)**

**Program Code No. 1E90K21
Investigators: W. Chiou, M. Aita,
A. Vitolo, and F. Pace
(516) 595-4211**

**Contractor:
AIL, a division of CUTLER-HAMMER
Deer Park, New York 11729**

**Scientific Officer:
Director, Physics Programs
Physical Science Division
Office of Naval Research**

**Effective Date of Contract: 1 June 1971
Contract Expiration Date: 31 May 1972
Amount of Contract: \$99,361**

**Sponsored by Advanced Research
Projects Agency, ARPA Order No. 306**

**This research was supported by the Advanced Research Project
Agency of the Department of Defense and was monitored by ONR
under Contract No. N00014-70-C-0161.**



TABLE OF CONTENTS

	<u>Page</u>
I Introduction	1
II Analytical Considerations on Parametric Image Upconversion with a Multimode Laser Pump	4
A. Geometric Optics Consideration	5
B. Physical Optics Consideration	10
III Material Damage and Light Absorption of Proustite at 1.06 μm	15
A. Material Damage	15
B. Light Absorption of Proustite at 1.06 μm	17
IV Evaluation of Varian Image Intensifier Tubes	21
V Imaging Experiments	28
VI Plans and Approaches for Second Half of Program	34
VII References	35

LIST OF ILLUSTRATIONS

<u>Figure</u>		<u>Page</u>
1	Geometry of Image Upconverter	6
2	Dark Noise Characteristics of a Varian Image Tube	22
3	Equivalent Noise Input and Radiant Gain of a Varian Image Tube	26
4	Experimental Arrangement for Parametric Image Upconversion	30
5	Intensity Plot of an Upconverted Image of Group 1 Bar Chart of USAF Resolution Target	31
6	Intensity Plot of an Upconverted Image of Group 2 Bar Chart of USAF Resolution Target	31

ABSTRACT

An experimental model imaging upconverter using a single-mode 5-W Nd:YAG laser as the pump source has been assembled and its imaging capability measured. A linear resolution of 112 lines along the horizontal direction was obtained. Resolution along vertical direction has not been measured quantitatively, but from symmetry considerations it should be comparable to the horizontal direction.

The dark noise characteristics of the GFE Varian image tubes were measured and found to be higher than anticipated. Attempts to use these tubes to demonstrate a real-time direct viewing capability were not successful because of the high tube dark noise and insufficient gain.

Pump laser damage to the nonlinear proustite material was considered. The bulk absorption coefficient of proustite at $1.06 \mu\text{m}$ was measured and found to be about 0.1 cm^{-1} for ordinary waves.

Imaging upconversion with a multimode laser pump was considered analytically. It was found that, as expected, transverse field distributions of the pump beam introduces spatial filtering effects.

I. INTRODUCTION

This is a semiannual technical report prepared under Contract N00014-70-C-0161 Modification P00003, entitled "10 Micrometer Detector," and having as its objective to develop an experimental model high resolution imaging upconverter for real-time direct viewing having 150 by 150 resolution elements and a NEP approaching $8 \times 10^{-11} \text{ W/Hz}^{1/2}$ under CW pumping condition.

A basic analytical model that describes parametric image upconversion was developed in the first phase of this program¹. Experiments were performed and analytical results were verified. Using 0.3-W CW Nd:YAG laser pump, resolution of 70 by 20 and power conversion of order of 10^{-7} were achieved in the first phase of the program.

In the present phase of the program, the main effort has been directed to develop an experimental model having 150 by 150 resolution elements and a NEP approaching $8 \times 10^{-11} \text{ W/Hz}^{1/2}$ using a 10-percent quantum efficiency image intensifier. To achieve this goal, a moderate power (5 watts) linearly polarized single-mode Nd:YAG laser was acquired and incorporated into the experimental setup. Also, three image tubes with 1-percent quantum efficiency at 967 nm were received from Varian Associates to be used for directly viewing the upconverted images². Imaging properties of the experimental system with the new pump laser have been evaluated during this reporting period.

In view of potential practical applications of parametric image upconversion as a range gated active IR imaging system, it has become apparent that the pump laser would be operated in the multimode manner and the nonlinear material would be pumped with a short-pulse high-intensity beam. Imaging with a multimode pump beam and laser damage effects on the nonlinear material are, therefore, important parameters to be investigated.

Parametric image upconversion with a multimode laser pump is considered analytically in Section II. Both a geometric optics approach and a physical optics technique are presented. The image position with respect to the locations of the objects and pump source is unaltered by the transverse mode structure of the pump source. It is shown that spatial filtering is introduced by transverse field distribution of pump beam. The results suggest possible application of spatial filtering techniques.

Section III discusses laser pump damage of the proustite crystal and the absorption measurement of proustite at $1.06 \mu\text{m}$. Possible damage mechanisms and a means for increasing the damage threshold are suggested. Light absorption of proustite at $1.06 \mu\text{m}$ was found to be 0.1 cm^{-1} for ordinary wave and 0.08 cm^{-1} for extraordinary wave. These values are one order of magnitude less than that at 694 nm of Ruby laser pumping³.

The noise characteristics of the GFE Varian image tubes were measured and are presented in Section IV. The dark noise was found to be relatively high and is not of thermal origin. Intermittent bright fluorescence is observed when the anode voltage exceeds 8 kV . Noise equivalent input (NEI)

of one tube was measured and was found to be two orders of magnitude worse than an estimated value based on the dark noise measurement. However, the NEI measurement was relatively crude and up to one order of magnitude of error is possible. Attempts to use the Varian image tubes to demonstrate direct viewing were not successful.

Section V presents resolution measurements of the experimental imaging system. Since a direct viewing device and image recording films were not available, the linespread function scanning technique with a slit-photomultiplier detector was used. A linear resolution of at least 112 lines in a 9-degree field along the horizontal direction was measured. Resolution along the orthogonal direction was not measured, but from symmetry considerations and only a small anisotropy it should not be very different. Measurements of conversion efficiency has been initiated. Efforts to improve the optical transmittance of the system components and suppressing some sources of noise are underway.

Section VI describes plans and approaches for the second half of this program.

II. ANALYTICAL CONSIDERATIONS ON PARAMETRIC IMAGE UPCONVERSION WITH A MULTIMODE LASER PUMP

Parametric image upconversion pumped by plane waves, spherical waves, and gaussian beams have been considered previously¹. It was shown that diffraction-limited resolution can be obtained under certain conditions. To make full use of the available pump laser power, it would be necessary to operate a pump laser in multimode pattern. The imaging properties of a system using a multimode pump laser are considered analytically in this section.

A geometric optics approach is presented in paragraph A of this section. A pump source with a circular aperture and uniform amplitude distribution is assumed. This simple model is necessary since geometric optics cannot handle the amplitude distribution. The analysis indicates that the extended pump source gives rise to an additional image blurring. Image degradation due to an extended pump source will disappear if, simultaneously, the nonlinear material is infinitesimally thin and the system is operating in the image space configuration. For a thick material, neglecting thickness aberration, it is shown that the circle of confusion due to an extended pump source is smaller (than that of the Fourier space configuration) by a factor of $(1 - \beta)$ for the image space configuration.

Physical optics considerations are presented in paragraph B of this section. The spatial frequency response (angular spectrum) of the up-converted image field is considered for two systems. In the first upconverter system, the nonlinear material is pumped by the near field of a TEM_{01} mode laser beam. The crystal in the second system is placed in the near field of a toroidal mode beam. The shape of the spatial frequency response resembles, as expected, that of pump field distribution. The result suggests possible spatial filtering technique for the upconversion system. Evaluation of the field distribution of upconverted image was not attempted at this time since it requires an extensive electronic computer effort.

A. GEOMETRIC OPTICS CONSIDERATION

It is assumed, for simplicity, that a uniform amplitude extended pump source is located at distance p from the nonlinear material (Figure 1). The pump source is assumed to have a circular aperture of radius b . This field distribution is not typical of the near-field distributions of a multimode laser beam, however, more complex field distributions can be expressed as linear sums of open resonator eigenmodes. We consider every source point within the source aperture as a point source radiating a spherical wave. Diffraction effects are neglected. It should also be noticed that the far-field distribution of laser beam with a uniform near-field distribution differs from the model considered.

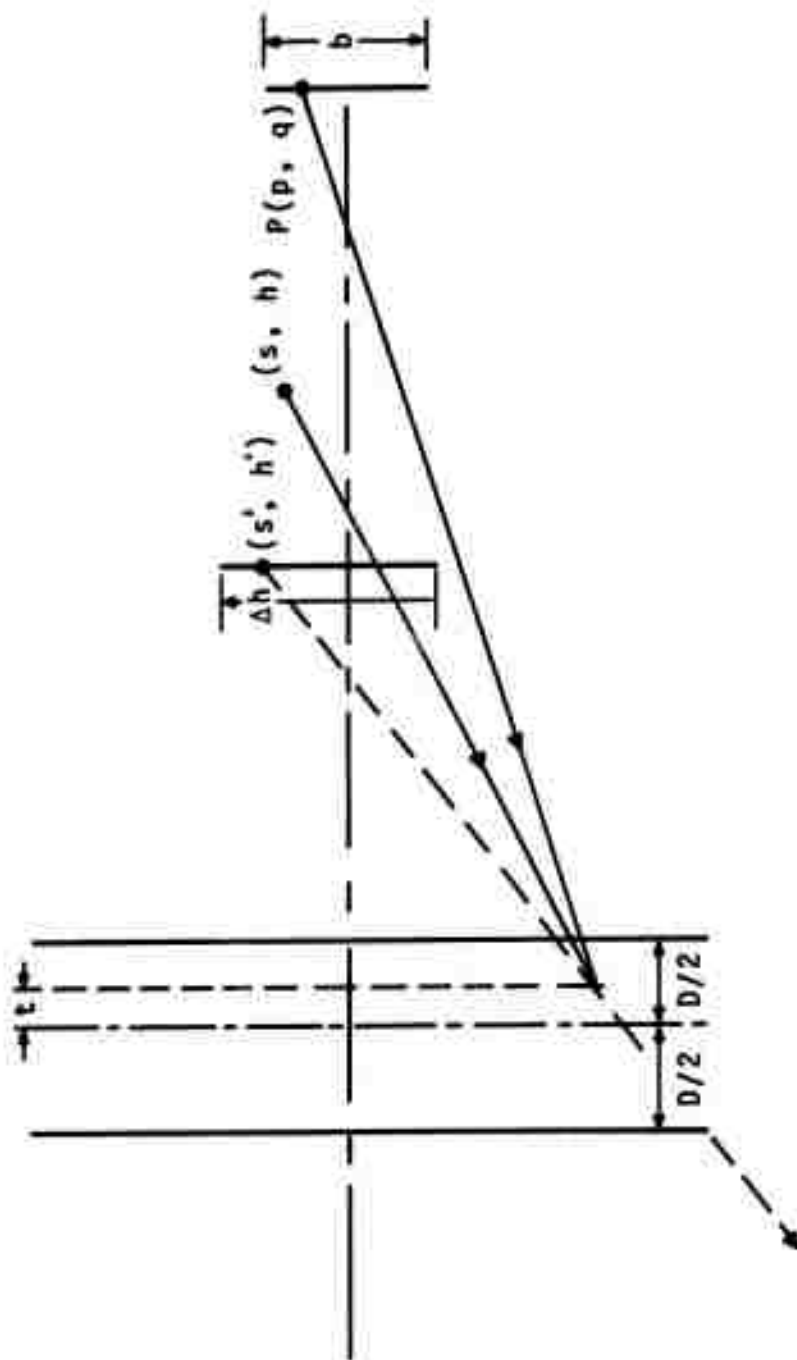


FIGURE 1. GEOMETRY OF IMAGE UPCONVERTER

Following the procedure described in previous report¹, the following image equations are obtained:

$$\left[n_s \left(s' + \frac{D}{2} \right) - \left(\frac{D}{2} + t \right) \right]^{-1} - \beta \left[n_i \left(s - \frac{D}{2} \right) + \left(\frac{D}{2} - t \right) \right]^{-1} = (1 - \beta) \left[n_p \left(p - \frac{D}{2} \right) + \left(\frac{D}{2} - t \right) \right]^{-1} \quad (1)$$

$$h' \left[n_s \left(s' + \frac{D}{2} \right) - \left(\frac{D}{2} + t \right) \right]^{-1} = h\beta \left[n_i \left(s - \frac{D}{2} \right) + \left(\frac{D}{2} - t \right) \right]^{-1} + q(1 - \beta) \left[n_p \left(p - \frac{D}{2} \right) + \left(\frac{D}{2} - t \right) \right]^{-1} \quad (2)$$

where

- D = thickness of nonlinear material
- n_l ($l = i, s, p$) = indices of refraction at λ_i , λ_s , and λ_p
- s = longitudinal distance of an infrared point object
- h = transverse distance of an infrared point object
- p = longitudinal distance of a point pump source
- q = transverse distance of a point pump source
- s' = longitudinal distance of a point image
- h' = transverse distance of a point image
- $\beta (= K_i/K_s)$ = angular demagnification factor
- t = longitudinal distance of interaction plane measured from the material center

Equation 1, which relates longitudinal distance of object, pump, and image, is independent of the pump transverse location.

For a very thin nonlinear material, such that the material thickness is negligible compared to other longitudinal distances, the equation relating transverse dimension becomes:

$$h' = [h + q s n_i (1 - \beta) / \beta p n_p] [1 + s n_i (1 - \beta) / \beta p n_p]^{-1} \quad (3)$$

Change in h' due to variation in q then becomes:

$$\Delta h' = \Delta q \frac{s n_i (1 - \beta)}{\beta p n_p + s n_i (1 - \beta)} \quad (4)$$

A point object at (s, h) interacting with an extended pump source of diameter b , thus, produces a circular upconverted image of diameter:

$$\Delta h' \bigg|_{D=0} = b \frac{s n_i (1 - \beta)}{\beta p n_p + s n_i (1 - \beta)} \quad (5)$$

The circle of confusion disappears if $s = 0$ or $p = \infty$. The case $s = 0$ represents image space interaction. It, however, can be noticed that the assumption $s \gg D$ becomes invalid when the condition $s = 0$ is approached.

When the material thickness is not negligible compared to other dimensions, the diameter of the circle of confusion becomes:

$$\Delta h' = b \frac{(1 - \beta) \left[n_i \left(s - \frac{D}{2} \right) + \left(\frac{D}{2} - t \right) \right]}{(1 - \beta) \left[n_i \left(s - \frac{D}{2} \right) + \left(\frac{D}{2} - t \right) \right] + \beta \left[n_p \left(p - \frac{D}{2} \right) + \left(\frac{D}{2} - t \right) \right]} \bigg|_{t = \frac{D}{2}}^{t = -\frac{D}{2}} \quad (6)$$

where $\Delta h'$ is evaluated at the limits $t = \frac{D}{2}$ and $t = -\frac{D}{2}$.

The additional confusion due to the thickness aberration is neglected in equation 6.

The circle of confusion disappears only if $p = \infty$. The circle of confusion for the image space configuration, where $s = 0$, becomes

$$\Delta h' \Big|_{s=0} = \frac{D b (1 - \beta)}{2} \left\{ \frac{1}{\beta \left[n_p \left(p - \frac{D}{2} \right) + D \right]} + \frac{1}{(1 - \beta) \left[\frac{D}{2} - \beta n_p \left(p - \frac{D}{2} \right) - (1 - \beta) \frac{D}{2} \right]} \right\} \quad (7)$$

Nonvanishing circle of confusion is apparently due to the thickness coma.

The circle of confusion for the Fourier space configuration, where $s = \infty$, becomes:

$$\Delta h' \Big|_{s=\infty} = b \quad (8)$$

As expected, the above relation, which holds for both thin and thick materials, indicates a plane wave pump is desired for the Fourier space interaction.

The circle of confusion for the image space configuration, $s = 0$, $p = 0$, becomes:

$$\Delta h' \Big|_{\substack{s=0 \\ p=0}} = b (1 - \beta) \quad (9)$$

The limiting resolution of a particular image upconversion system can be calculated by the procedure described in the preceding report.

The image blurring due to the aberration and the circle of confusion introduced by the pump divergence (extended pump source) are, however, not simply additive. The geometry of image formation must be carefully examined for an individual system. While the thickness aberration may completely override the blurring due to the divergent pump for a certain system, it is possible that the effect of pump divergence is dominant for another system.

B. PHYSICAL OPTICS CONSIDERATION

Consider first the case of a TEM_{01} mode pump laser beam.

Assume that the material is placed in the near field (the waist) of the beam. The field distribution of the pump beam can be considered as an optical window for IR object waves. The near-field distribution of a TEM_{01} mode beam is expressed⁴, in a cylindrical coordinate system as,

$$E_{01}(\zeta) = \left(1 - 2 \frac{\zeta^2}{a^2}\right) \exp\left(\frac{-\zeta^2}{a^2}\right) \quad (10)$$

where

ζ = radial coordinate

a = beam radius of fundamental mode

Unity amplitude is assumed in equation 10 for simplicity. The angular spectrum of a TEM_{01} field distribution is the Hankel transform of field distribution given by equation 10,

$$\mathcal{E}_{01}(\kappa) \sim \int_0^\infty \left(1 - 2 \frac{\zeta^2}{a^2}\right) \exp\left(\frac{-\zeta^2}{a^2}\right) J_0(\kappa \zeta) \zeta d\zeta \quad (11)$$

It can be shown that $\mathcal{G}_{01}(K)$, neglecting a constant multiplicative factor, becomes

$$\mathcal{G}_{01} \sim \frac{a^2}{2} \left(\frac{a^2 \kappa^2}{2} - 1 \right) \exp \left(\frac{-a^2 \kappa^2}{4} \right) \quad (12)$$

Neglecting double refraction effects and following the procedure developed previously¹, it can be shown that the equation relating the image position and the object position is identical to that of gaussian beam pumped case. The angular spectrum of upconverted field distribution over the image plane for an on-axis point object again neglecting constant multiplicative factors, is given by:

$$\mathcal{G}_s(\kappa_s, s') \sim \frac{\sin(\Delta \kappa D/2)}{(\Delta \kappa D/2)} \int \frac{a^2}{2} \left(\frac{a^2 \kappa^2}{2} - 1 \right) \exp \left[-\left(\frac{a^2}{4} + i \frac{\alpha}{2} \right) \kappa^2 \right] \cdot \exp \left[-i\alpha \underline{\kappa}_s \cdot \underline{\kappa} \right] d\underline{\kappa} \quad (13)$$

where $\alpha = \lambda_i (s - 2/D)/2\pi$

The $(\sin x/x)$ function arises again from phase mismatch for a given angular spectrum. The attenuation factor expressed by the integration in equation 13 is due to the transverse mode structure of the pump laser beam. The attenuation factor,

$$I_{01} = \frac{a^2}{2} \int \left(\frac{a^2 \kappa^2}{2} - 1 \right) \exp \left[-\left(\frac{a^2}{4} + i \frac{\alpha}{2} \right) \kappa^2 \right] \exp \left[-i\alpha \underline{\kappa}_s \cdot \underline{\kappa} \right] d\underline{\kappa}$$

can be rewritten as Hankel transform,

$$I_{01} = \frac{a^2}{2} \int \left(\frac{a^2 \kappa^2}{2} - 1 \right) \exp \left[- \left(\frac{a^2}{4} + i \frac{\alpha}{2} \right) \kappa^2 \right] J_0 (\alpha \kappa_s \kappa) \kappa d\kappa$$

Evaluating the integration, we obtain

$$I_{01} = a^2 \frac{\exp \left(- \frac{\alpha^2 \kappa_s^2}{a^2 + i2\alpha} \right)}{(a^2 + i2\alpha)^3} \left(a^4 + 4\alpha^2 - 2\alpha^2 a^2 \kappa_s^2 \right) \quad (14)$$

If the condition $a^2 \gg 2\alpha$ is satisfied, equation 14 becomes:

$$I_{01} = \left(1 - 2 \frac{\alpha^2}{a^2} \kappa_s^2 \right) \exp \left(-\alpha^2 \kappa_s^2 / a^2 \right) \quad (15)$$

Equations 14 and 15 indicate that the image spectrum at high spatial frequencies of the TEM_{01} beam pumped image upconverter system is attenuated more than that of gaussian beam pumped system.

We consider, next, an upconverter system pumped by a toroidal mode laser beam. The toroidal mode, the simplest multimode distribution, considered here is produced by subtracting equal amplitude TEM_{01} mode field from TEM_{00} mode field. The near-field distribution of this mode is expressed by:

$$E_D (\zeta) = E_{00} (\zeta) - E_{01} (\zeta) = 2 \frac{\zeta^2}{a^2} \exp \left(-\frac{\zeta^2}{a^2} \right) \quad (16)$$

The angular spectrum of the toroidal field distribution is:

$$G_D(\kappa) \sim a^2 \left(1 - \frac{a^2 \kappa^2}{4} \right) \exp \left(\frac{-a^2 \kappa^2}{4} \right) \quad (17)$$

It can be shown that the mode attenuation factor for the angular spectrum of the upconverted image field produced by this system is

$$I_d = \frac{2a^2}{(a^2 + i2\alpha)^3} \left[a^2 \alpha^2 \kappa_s^2 + i2\alpha (a^2 + i2\alpha) \right] \exp \left[\frac{-\alpha^2 \kappa_s^2}{(a^2 + i2\alpha)} \right] \quad (18)$$

Again for the condition $a^2 \gg 2\alpha$, the attenuation factor I_d approaches

$$I_d \sim \left(\frac{\alpha^2}{a^2} \kappa_s^2 + i \frac{4\alpha}{a^2} \right) \exp \left(\frac{-\alpha^2 \kappa_s^2}{a^2} \right) \quad (19)$$

For $\kappa_s^2 \gg |4/\alpha|$,

$$I_d \sim \frac{\alpha^2}{a^2} \kappa_s^2 \exp \left(\frac{-\alpha^2 \kappa_s^2}{a^2} \right) \quad (20)$$

Equations 19 and 20 indicate that a relative high spatial frequency enhancement takes place with the toroidal mode pumping. The dc frequency spatial component is decreased and the peak frequency response shifted to higher frequencies.

The above results strongly suggest that spatial filtering can be performed by properly shaping the pump beam. Many techniques developed for

optical data processing and holography can be applied directly to the parametric image upconverter if the pump beam shape is predictable and stable.

The above computational technique can be applied to any TEM_{0n} ($n = 0, 1, 2, \dots$) mode pump beam. It is, however, expected that the mode attenuation factor for circularly asymmetrical modes will not be expressable in a closed form.

III. MATERIAL DAMAGE AND LIGHT ABSORPTION OF PROUSTITE AT $1.06\ \mu\text{m}$

A. MATERIAL DAMAGE

The question of material damage is central to the design and operation of a parametric upconversion systems; the reason being the large pump radiation power densities to which the nonlinear materials are subjected for attaining high conversion efficiency.

Damage thresholds of the proustite crystal under different conditions have been reported by many authors. Fountain et al⁵ reported on damage thresholds of proustite at $1.06\ \mu\text{m}$ subjected both to CW irradiation and a Q-switched laser pulse. They ascribed damage in proustite to local heating caused by absorption. Hanna et al⁶ also published their results of Q-switched laser damage of proustite crystals at $1.06\ \mu\text{m}$, $10.6\ \mu\text{m}$, and $694\ \text{nm}$. The damage thresholds of Q-switched laser irradiation at $1.06\ \mu\text{m}$ reported by Fountain and Hanna are comparable. Hanna, however, excluded surface melting due to absorption as a probable damage mechanism. Lucy⁷ has also reported damage threshold of proustite with a pulsed Ruby laser. He observed significant damage at peak power densities of $10\ \text{kW}/\text{cm}^2$ with 1-ms pulse. This level is three orders of magnitude below those reported by Hanna with a Q-switched Ruby laser. Accumulation of damage is apparent from these data.

The three cited references have not reached a clear correlation between damage thresholds and bulk-absorption coefficients. They disagreed on a probable damage mechanism.

At AIL the upconversion system has been operated by pumping the proustite crystal with CW Nd:YAG laser radiation. An accumulation of white powder on the exit surface of proustite crystal has been noticed. This may be attributed to radiation enhanced surface oxidation^{6, 8}. The area and shape of powder accumulation matches the 1.06- μ m beam cross section. The powder accumulation is noticeable after a few tens of minutes of continuous irradiation at approximately 1 W/cm². Warner⁹ indicated the same phenomenon with a continuous 694-nm irradiation of proustite. He reported that the surface oxidation becomes visible after several minutes of 694-nm irradiation at approximately 1 W/cm².

In an attempt to obtain more information on the surface oxidation of proustite, an experiment was performed by placing a proustite in an evacuated vessel. The vessel was evacuated to approximately one Torr pressure and the crystal was irradiated with a chopped 1.06- μ m beam of 80-percent duty factor. The average power density of 1.06- μ m beam was approximately 3 W/cm² with a temporal peak power density of 37.5 W/cm². Surface oxidation was not observed even after 1/2 hour of irradiation. This level of exposure is considerably higher than the level proustite would tolerate in the atmosphere. The result indicates that Q-switched laser damage threshold of proustite might be improved if the proustite is operated in a vacuum or in an inert gas atmosphere.

B. LIGHT ABSORPTION OF PROUSTITE AT 1.06 μm

The correlation between damage thresholds and bulk light absorption is not clearly understood. There are, however, data that indicate that the damage thresholds and surface oxidation levels of proustite are lower at 694 nm than at 1.06 μm . Lower damage threshold at 694 nm may be attributed to higher light absorption. Therefore, it has been found to be worthwhile to obtain the light absorption coefficient of proustite at 1.06 μm , since bulk absorption of proustite at 1.06 μm has never been reported in literature.

A calorimetric measurement was done of the absorption coefficients of a proustite crystal prepared for upconversion of 10.6- μm infrared radiation to 967 nm. * The crystal is oriented such that the optic axis (C-axis) makes a 20-degree angle with the normal of the (polished) front surface. The crystallographic X-axis is parallel to the front surface. A linearly polarized chopped 1.06- μm beam from a CW TEM₀₀ mode Nd:YAG laser was incident normally on the crystal front surface. The average power densities at the center of 1.06- μm beam were approximately 5 W/cm². The duty factor of light chopper is 8.5 percent and the repetition period is short enough to neglect the thermal time constant of the material.

* Measurements were performed with an absorption meter at Holobeam Inc., Paramus, N. J.

The average power level incident on the crystal, the average power transmitted through the material, and the average power absorbed by the crystal were measured. The proustite was mounted on a Peltier cooler. Electric current through the Peltier cooler was adjusted until an equilibrium was reached between the heat generated by the crystal light absorption and the cooling rate of the Peltier cooler. The amount of light power absorbed by a material is, thus, measured by observing the cooling current of the calibrated Peltier cooler.

Absorptions of the ordinary wave, which is polarized normal to the crystal C-axis, and of the extraordinary wave, which is polarized parallel to the C-axis, were measured. Reflection losses at the surfaces were calculated from the Fresnel reflection formula since the index of refraction of proustite is accurately known. Table I lists the measured power levels and the percentage power level referred to the input power.

TABLE I. TRANSMISSION AND ABSORPTION OF A
0.95-CM LONG PROUSTITE* AT $1.06\ \mu\text{M}$

	<u>Incident Average Power</u>		<u>Transmitted Power</u>		<u>Absorbed Power</u>		<u>Calculated Re- flection Loss</u>
	mW	percent	mW	percent	mW	percent	percent
Ordinary Wave	153.5	100	77.4	50.5	11.1	7.24	40.2
Extraordinary Wave	160	100	82.6	51.6	9.6	6.0	38.2

* Proustite is prepared for type II upconversion of $10.6\ \mu\text{m}$ with the $1.06\text{-}\mu\text{m}$ pump.

As evident from Table I, 2 percent of incident power for the ordinary wave case and 4 percent for the extraordinary wave case are unaccounted for. While it is possible that this missing power is due to the measurement error, it was felt that the scattering inside the crystal is responsible for the bulk of these losses. The accuracy of the power absorption measurement is, according to J. Muray of Holobeam, within ± 5 percent of actual.

The absorption coefficient of the material was computed by the following equation:

$$P_{ab} = P_o (1 - e^{-\alpha l}) \quad (21)$$

where,

P_{ab} = absorbed power

P_o = power input to the material, excluding the front surface reflection loss

α = absorption coefficient

l = material length in cm

The absorption coefficient for the ordinary wave was found to be 0.104 cm^{-1} and that for the extraordinary wave is 0.082 cm^{-1} . The measured absorption coefficients at $1.06 \mu\text{m}$ are one order of magnitude less than that reported at 694 nm^3 .

During the absorption measurement, a slight reversible temperature dependent absorption was noted. Quantitative measurements of the temperature dependence were not performed because of limitations in the instrument.

Light absorption of proustite at $1.06 \mu\text{m}$ is slightly less than the 0.45 cm^{-1} for pyrargyrite¹⁰ and is considerably better than that of ZnGeP_2 ¹¹, selenium, and CdGeAs_2 ¹².

The temperature dependence of the light absorption and the thermal properties of the proustite should be measured to provide a better understanding of damage mechanism. It is also recommended that a more extensive and more thorough investigation of the laser damage of proustite be done under controlled conditions.

IV. EVALUATION OF VARIAN IMAGE INTENSIFIER TUBES

Three image tubes using InAsP transmission photocathodes developed by Varian Associates² were received GFE by AIL. The quantum efficiency of the photocathode is approximately 1 percent and is considerably lower than the anticipated 10 percent efficiency. Since no extensive investigation of background noise was undertaken at Varian, the noise characteristics of received tubes were measured at AIL.

A voltage breakdown occurred inside one of the tubes when the anode voltage was raised to 12 kV. The tube that experienced breakdown ceased functioning afterward. Intermittent fluorescence on the output phosphor of the second tube was observed after a few hours of operation. The fluorescence becomes visible when the anode voltage exceeds 8 kV.

The output phosphor screen of one of the tubes was imaged, with a relay lens, onto the photocathode of a calibrated photomultiplier. Electrical output of the photomultiplier tube is then connected to an electronic counter. Both the Varian tube and the photomultiplier tube were placed in a light shielded box. The anode voltage of the tube was varied and corresponding photomultiplier output was recorded. The measured result is plotted in Figure 2. The larger data spread at higher anode voltage is probably due to intermittent fluorescence of output phosphor of tested tube. The steep increase of the dark noise output of the tube indicates that the dark noise is

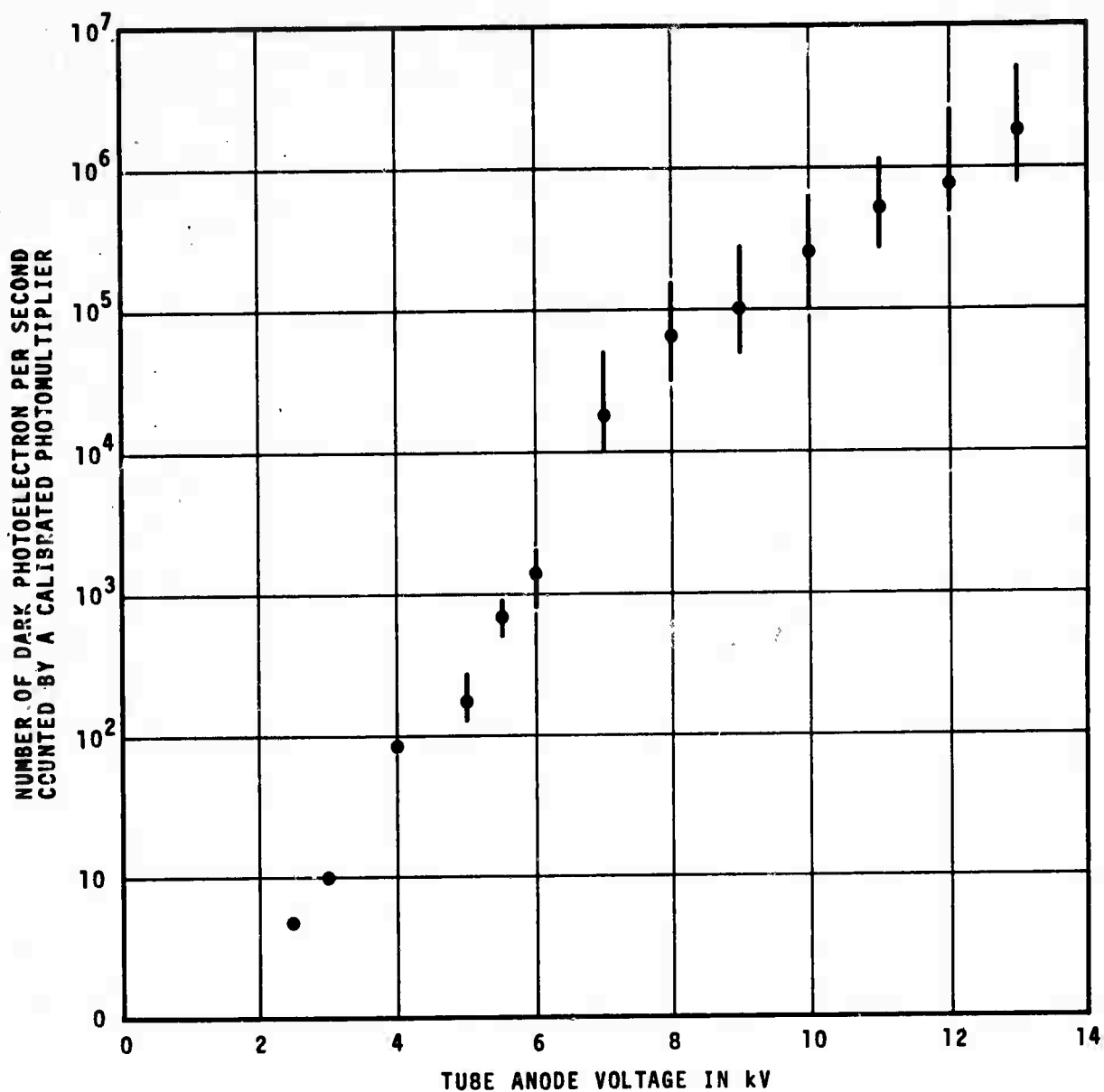


FIGURE 2. DARK NOISE CHARACTERISTICS OF A VARIAN IMAGE TUBE

not of thermionic origin. R. Bell of Varian indicated that it could be due to internal luminescence excited by leakage currents through the bulk or over the surface of the insulators, or by electron bombardment of the internal surfaces by electrons field-emitted from the cathode holder or focus electrode².

Dark noise radiant emittance from the phosphor surface of a tube is calculated by a formula:

$$W_d = \frac{4 (1 + M^2) F^2 hc}{T \eta_D \lambda_o A_D} N_d \quad (22)$$

where

W_d = dark noise radiant emittance from the output phosphor
in W/cm^2

F = F number of the relay lens

M = magnification factor of the relay lens

h = Planck's constant

c = speed of light

N_d = photoelectron count of the photomultiplier tube in Hz

T = transmission through the relay lens and other intervening components

η_D = photocathode quantum efficiency of the photomultiplier tube

λ_o = wavelength of peak radiation of output phosphor of the image tube in cm

A_D = effect of collective aperture of the photocathode of the photomultiplier

Using parameter values of $\eta_D = 0.08$, $F = 2.35$, $M = 1$, $\lambda_o = 0.55 \times 10^{-4}$ cm, $A_D = 0.28 \text{ cm}^2$, and $T = 0.66$, the dark noise radiant emittance is expressed as a function of photoelectron count of the photomultiplier,

$$W_d = 1.08 \times 10^{-15} N_d W/\text{cm}^2 \quad (23)$$

Radiant power gain of a single stage image intensifier tube is expressed approximately by:

$$G(\lambda_i) = \frac{W_o}{W_i(\lambda_i)} \approx \eta_o \eta_c \frac{A_c}{A_o} \frac{\lambda_i}{hc} V \times 1.602 \times 10^{-19} \quad (24)$$

where

η_o = quantum efficiency of output phosphor

η_c = quantum efficiency of input photosurface at λ_i

A_c = aperture area of input photosurface

A_o = aperture area of output phosphor

V = effective accelerating voltage

Using known parameter values $\eta_o = 0.05$, $\eta_c = 0.01$, and $A_c/A_o = 1$, the gain of Varian image tube is given by:

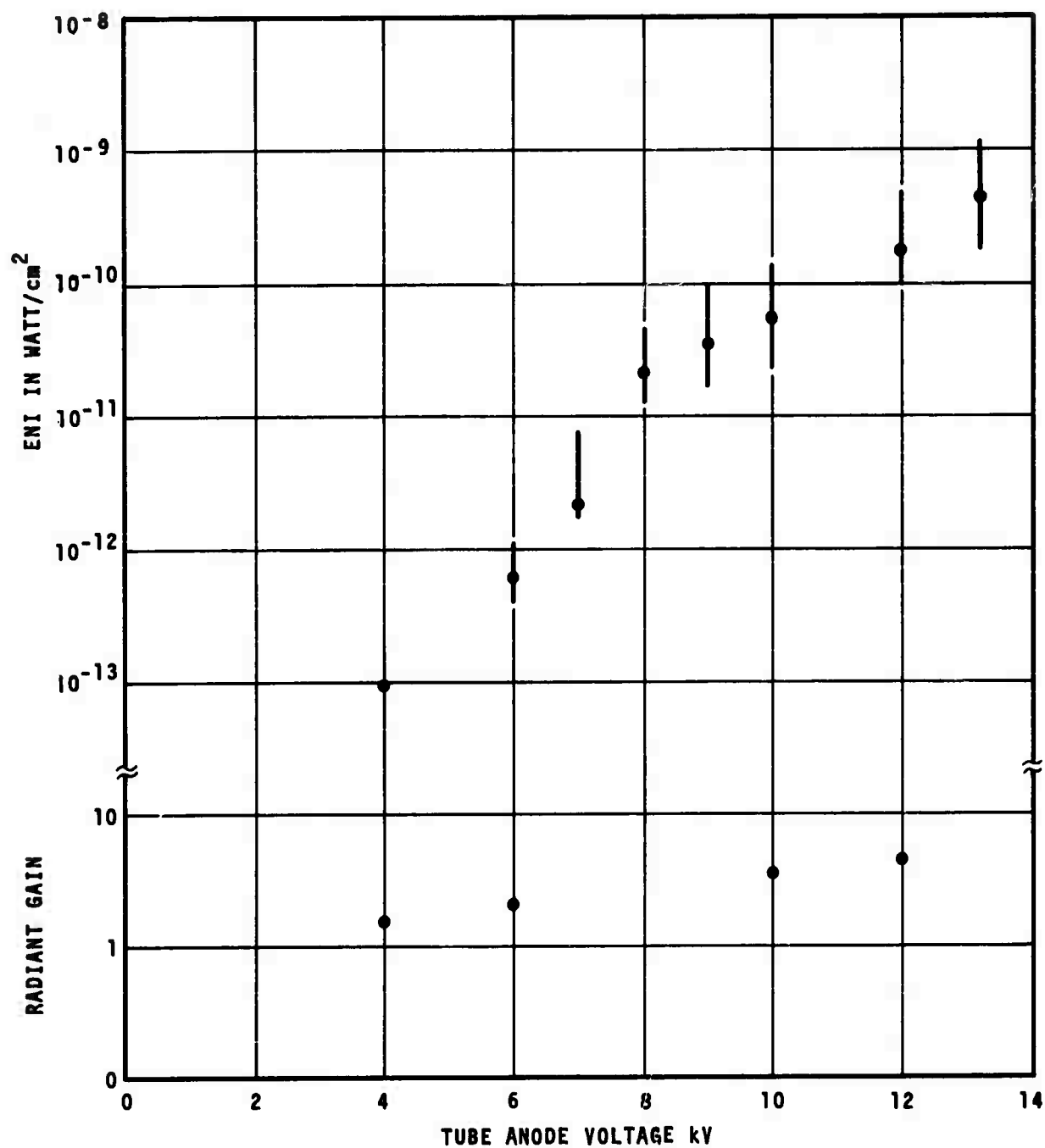
$$G(0.95 \mu m) = 3.8 \times 10^{-4} \text{ V} \quad (25)$$

Combining equations 23 and 25, the following expression for noise equivalent irradiance (NEI) of the Varian tube tested is obtained:

$$H_d = \frac{W_d}{G} = 2.84 \times 10^{-12} \frac{N_d}{V} \text{ W/cm}^2 \quad (26)$$

Figure 3 is a plot of predicted NEI as a function of anode voltage of the tube tested. Radiant gain at $0.95 \mu m$ of the Varian tube with 1 percent photocathode efficiency is also plotted in Figure 3.

Attempts to measure the radiant gain and the EBI of the Varian tubes were not quite successful because of the intermittent fluorescence of the output phosphor. A laser diode of known radiance at $0.96 \mu m$ was used to illuminate the photosurface of a Varian tube and a 960-nm interference filter of known transmittance was placed in front of the Varian tube. Light output from the phosphor surface was measured by the relay lens photomultiplier combination. Bright intermittent fluorescence overrode the signal and prevented the taking of meaningful data. An approximate sensitivity was determined by visually observing the output phosphor of the tube while the distance between the light emitting diode and the image tube was altered. The distance was noted when the signal from the output phosphor of the tube



2-1843

**FIGURE 3. EQUIVALENT NOISE INPUT AND RADIANT GAIN OF A
VARIAN IMAGE TUBE**

tested becomes detectable by the naked eye. The minimum discernable irradiance on the photosurface of the tube was about 10^{-6} W/cm^2 for a 10-kV anode voltage. Assuming $2 \times 10^{-10} \text{ W/cm}^2$ background radiant emittance for the output phosphor and the minimum detectable brightness of 10^{-3} foot-lambert¹³ (corresponding to 10^{10} photons/cm²) for an ordinary eye, the radiant NEI of tested tube is estimated to be in the order of 10^{-8} W/cm^2 .

One of Varian tubes was incorporated into the experimental image upconverter system to demonstrate a direct viewing real-time capability. Because of the low gain and relatively high noise, we have not been able to observe a visual image of the $10.6\text{-}\mu\text{m}$ illuminated objects.

A gated three-stage image intensifier tube with S1 photosurface, 10^{-9} W/cm^2 EBI, and the radiant gain of 200 will be used in the system to achieve real-time direct viewing capability. Since typical quantum efficiency of S1 photosurface is about 0.2 percent, two orders of magnitude degradation in sensitivity from the objective of $8 \times 10^{-11} \text{ W/Hz}^{1/2}$ with 10 percent image tube is expected.

V. IMAGING EXPERIMENTS

The number of resolution elements contained in upconverted images is proportional to the effective interaction aperture. It has also been shown that, for optimum resolution, the beam diameter of a Gaussian pump beam should be considerably larger than the object aperture subtended by the acceptance angle of upconversion process. It is also known that the system conversion efficiency is inversely proportional to the effective interaction aperture for a given pump power. High pump power is, therefore, essential for sensitive high resolution image upconversion system as depicted in the following expression:

$$\eta N \sim \theta^2 P_p$$

where

η = power conversion efficiency

N = number of resolution elements in an image

θ = input signal acceptance angle

P_p = pump power

A linearly polarized medium power Nd:YAG laser operating in TEM₀₀ mode was obtained for the program. The power output of the pump laser operating in a linearly polarized TEM₀₀ mode is about 5.5 watts. The beam divergence is about 0.7 mrad and the beam diameter is approximately 2 mm. The pump

beam is expanded and collimated by a beam expander. The beam spot diameter at the proustite is 8.5 mm, and the total power of the pump beam impinging on the proustite is 5 watts. Using a formula

$$W_{\max} = 2P/A_p$$

where

W_{\max} = spatial peak power density

P = total beam power

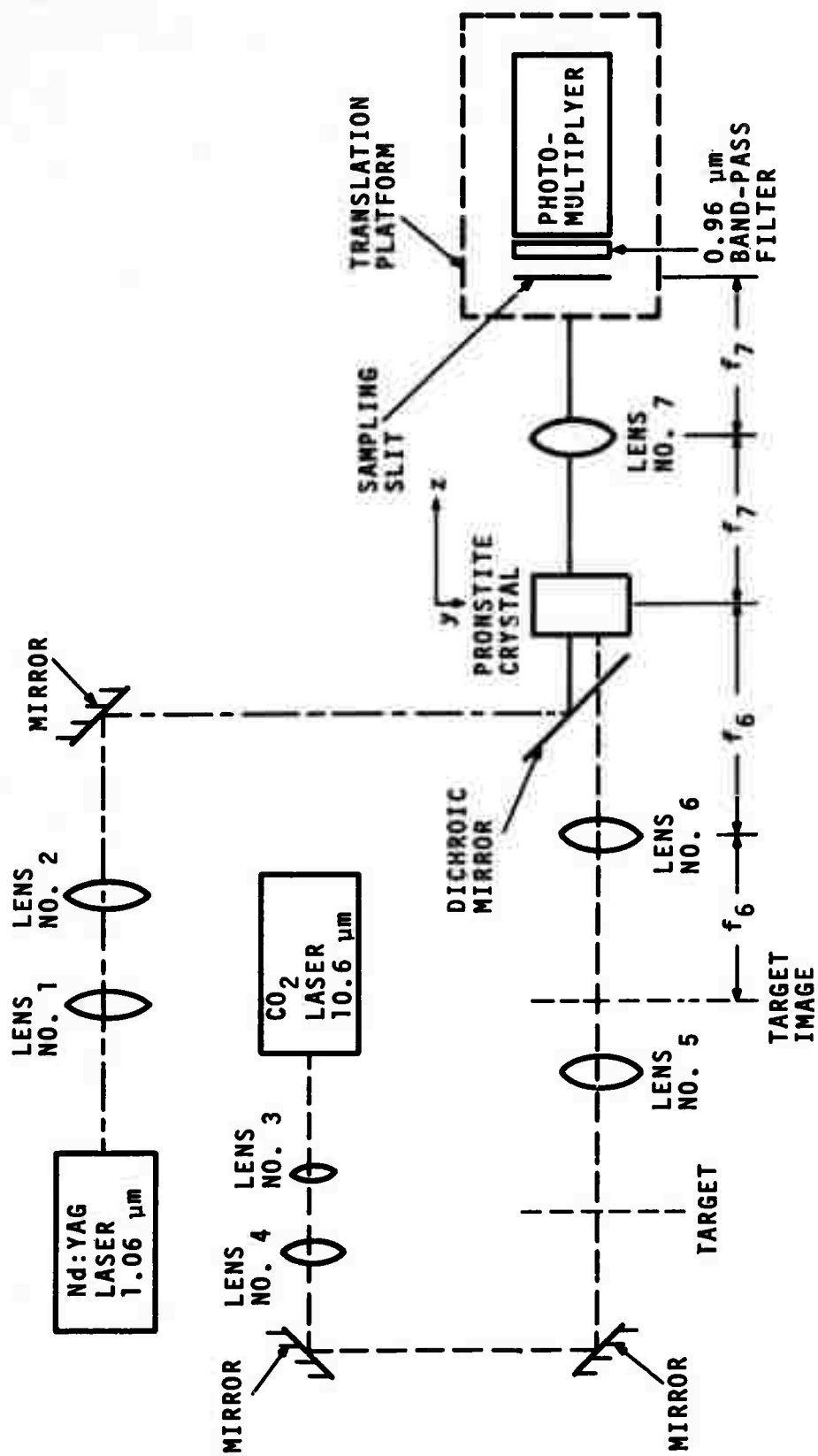
A_p = area of beam waist

we found

$$W_{\max} = 17 \text{ W/cm}^2$$

A check was made to confirm Gaussian shape of the pump beam intensity distribution.

Image experiments were carried out in the Fourier space configuration. Figure 4 shows a schematic drawing of the experimental setup. A resolution target was back illuminated by 10.6- μm laser beam and was imaged on the front focal plane of lens No. 6 by lens No. 5. Lens No. 5 has a 2.3 \times magnification. Focal length of lens No. 6 and lens No. 7 is 12 and 50 cm, respectively. The intensity profile of upconverted images were probed by a slit-photomultiplier combination. Figure 5 shows a measured intensity profile of upconverted image of group 1 bar chart of the 1951 USAF resolution target. Figure 6 is a measured intensity distribution of upconverted image



2-1844

FIGURE 4. EXPERIMENTAL ARRANGEMENT FOR PARAMETRIC IMAGE UPCONVERSION

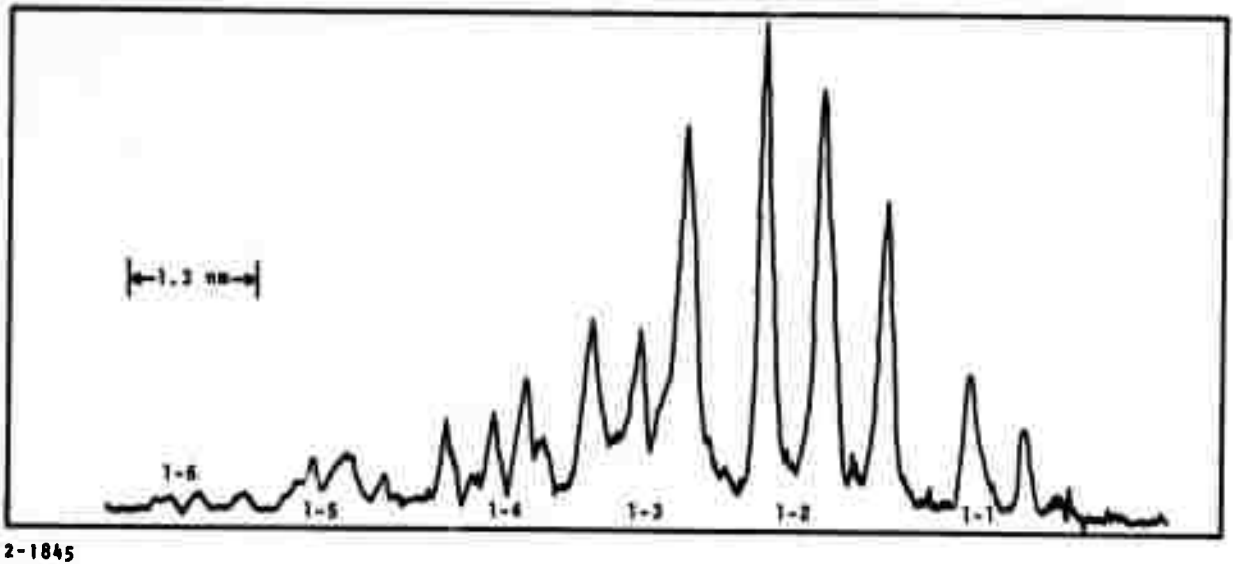


FIGURE 5. INTENSITY PLOT OF AN UP CONVERTED IMAGE OF GROUP 1 BAR CHART OF USAF RESOLUTION TARGET

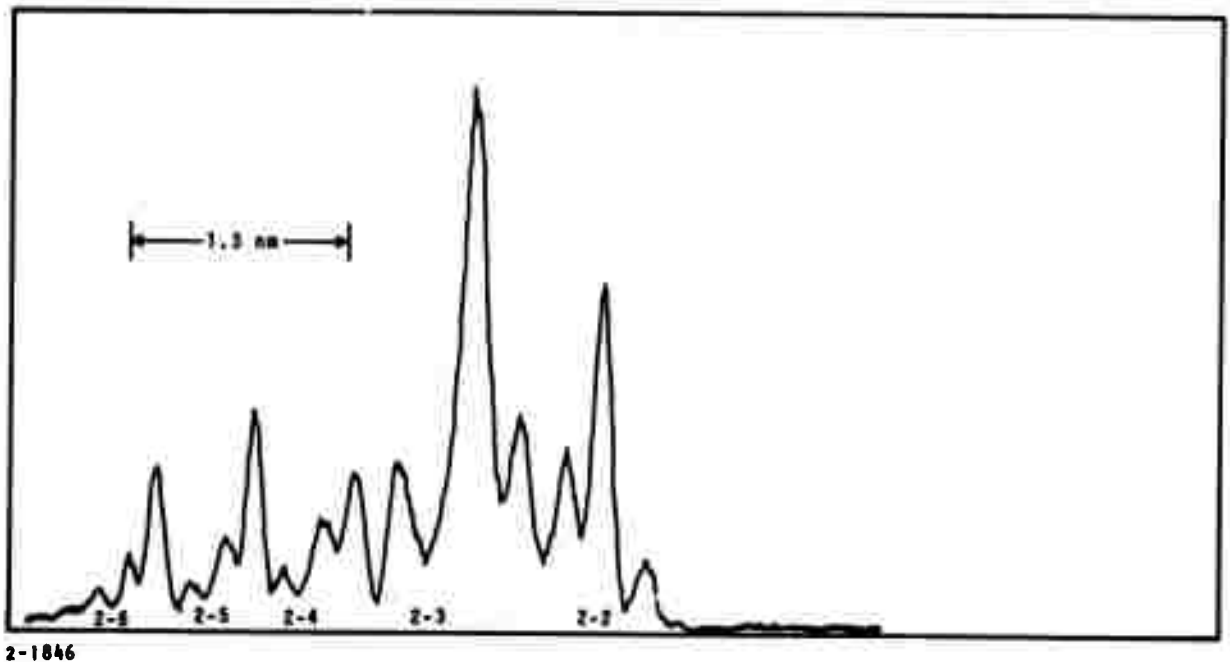


FIGURE 6. INTENSITY PLOT OF AN UP CONVERTED IMAGE OF GROUP 2 BAR CHART OF USAF RESOLUTION TARGET

of group 2 bar chart of the resolution target. It can be seen clearly that bars in the target 2-6, which has a period of 7.13 line-pair per millimeter are resolved. Taking the width of group 1 bar chart of 8 mm as the maximum object width and the spatial frequency of 7.13 line pair/mm as the maximum resolvable frequency, we found that an upconverted image will contain at least 112 lines along the horizontal direction. No attempt was made to make similar measurement along vertical direction.

The extreme angle which the $10.6\ \mu\text{m}$ object ray subtends at the input surface of the proustite is about 4.5 degrees, which is well within the acceptance angle of the upconverter used. It is believed that the number of resolution elements can be increased to 140 lines when the full 12-degree acceptance angle is used.

An attempt was made to use a Varian image tube to observe images at 967 nm, but it was not successful because of poor signal-to-noise ratio and low radiant gain.

Recording of the 967-nm images on IR films was not performed because Kodak discontinued manufacturing of Type I-M spectroscopic film and none is available from stock.

Sensitivity measurements have been initiated, but no reportable results have been obtained as of this writing. Preliminary power measurements, however, indicates the increase of conversion efficiency by at least a factor of five from that of former systems which used an 0.3-W pump

power. The objective of the sensitivity measurement in the present program is to resolve the discrepancy existing between the experimental result and the simple theory and formulate a more accurate computational model.

VI. PLANS AND APPROACHES FOR SECOND HALF OF PROGRAM

The effort for the second half of this program will be directed toward:

- Development of a direct viewing image upconverter
- Measurement of conversion efficiency of the imaging system
- To develop a better model for imaging conversion efficiency calculation and to compare with the efficiency measurement
- Improvement of optical efficiency of optical components

A gated three-stage image intensifier tube with S1 photosurface will be incorporated in the system for demonstration of a direct viewing imaging system. Since typical quantum efficiency of S1 photosurface is about 0.2 percent, the optimum NEP of the experimental direct viewing system will be in the order of $10^{-10} \text{ W/Hz}^{1/2}$ under CW pumping condition. Conversion efficiency of the experimental model which uses Gaussian beam pump will be first measured and compared with analytical calculation. Single resolution element NEP of the direct viewing system will be measured.

VII. REFERENCES

1. W. Chiou and F. Pace, "Research on Imaging Properties of Optical Parametric Upconverter," AIL Report 8585-1, prepared under Contract N00014-70-C-0161, ARPA Order No. 306, July 1971.
2. Ron Bell, "Photo-Emissive Detector," Final Report, Varian Associates, prepared under Contract N00014-17-C-00173, ARPA Order No. 306, August 1970.
3. K. Hulme, O. Jones, P. Davis, and M. Hobden, "Synthetic Proustite: A New Crystal for Optical Mixing," Appl Phys Letters 10, 133, 15 February 1967.
4. H. Kogelnik and T. Li, "Laser Beams and Resonators," Appl Optics 5, p 1550, 1960.
5. W. Fountain, L. Osterink, and G. Massey, "Optically Induced Physical Damage to LiNbO_3 , Proustite and LiIO_3 ," Proc Conf, Damage in Laser Materials, Boulder, Colorado, May 1971.
6. D. Hanna, B. Davies, H. Rutt, R. Smith, and C. Stanley, "Q-Switched Laser Damage of Infrared Nonlinear Materials," IEEE Jour of QE, QE-8, p 317, 1972.
7. R. Lucy, "Laser Parametric Image Upconversion," Tech Rep AFAL-TR-72-23, Itek Corporation, January 1972.
8. P. H. Pough, "A Field Guide to Rocks and Minerals," London, Constable, 1970.
9. J. Warner, Private communication.
10. J. Feichtner, R. Johannes, and G. Roland, "Growth and Optical Properties of Single Crystal Pyrargyrite (Ag_3SbS_3)," Appl Optics, Vol 9, p 1716, 1970.
11. G. Boyd, W. Gandrud, and E. Buehler, "Phase-Matched Upconversion of $10.6\text{ }\mu\text{m}$ Radiation in ZnGeP_2 ," Appl Phys Letters, Vol 18, p 446, 15 May 1971.

12. R. Byer, H. Kildal, and R. S. Feigelson, "CdGeAs₂: A New Non-linear Crystal Phasematchable at 10.6 μ m," Appl Phys Letters, Vol 19, p 237, 1 October 1971.
13. A. Rose, "Quantum Limitation to Vision at Low Light Levels," in Proc Seminar Low Light Level Imaging Systems, N.Y., March 1970.